SCIENTIFIC REP🞜RTS

Finite-temperature scaling of trace distance discord near criticality in spin diamond structure

W. W. Cheng[1], X. Y. Wang[1], Y. B. Sheng[1], L. Y. Gong[1,2], S. M. Zhao[1] & J. M. Liu[2]

In this work we explore the quantum correlation quantified by trace distance discord as a measure to analyze the quantum critical behaviors in the Ising-XXZ diamond structure at finite temperatures. It is found that the first-order derivative of the trace distance discord exhibits a maximum around the critical point at finite temperatures. By analyzing the finite-temperature scaling behavior, we show that such a quantum correlation can detect exactly the quantum phase transitions from the entangled state in ferrimagnetic phase to an unentangled state in ferrimagnetic phase or to an unentangled state in ferromagnetic phase. The results also indicate that the above two kinds of transitions can be distinguished by the different finite-temperature scaling behaviors. Moreover, we find that the trace distance discord, in contrast to other typical quantum correlations (e.g., concurrence, quantum discord and Hellinger distance), may be more reliable to exactly spotlight the critical points of this model at finite temperatures under certain situations.

For a quantum many-body system, the ground state properties may undergo qualitative and dramatic changes owing to quantum fluctuations at zero temperature. This phenomenon, known as a quantum phase transition (QPT), is attributed to the interplay between the different orders associated with competing interactions in the Hamiltonian[1]. However, the QPT can also emerge and be observed at sufficiently low temperature if thermal fluctuations are not sufficient to drive the system away from its ground state to excited states. In the other words, the quantum fluctuations still dominate at these temperatures. Recently, the finite-temperature properties of QPT have been attracting attention due to the fact that all experiments are confined to finite temperature[2–4]. Thus, an understanding of only the zero-temperature properties of a quantum system is not sufficient from the perspective of experimental results.

On the other hand, quantum correlations among the subsystems of a many-body system are closely related to the emergence of the QPT. In recent years, such relationships have been studied from many different perspectives in varies quantum systems[5–22]. For instance, entanglement has been widely employed to identify QPT with great success[7–20]. However, entanglement may fail to measure the quantum correlations for a state in some specific cases (e.g., the case with remote spin pairs in a spin chain system[8]). That's to say, there exist other quantum correlations which can not be grasped by entanglement. In addition, entanglement might signal a pseudo transition point[18]. These facts stimulate many works to classify and quantitate the quantum correlations from other perspectives in order to avoid this disadvantage[23–29]. In particular, Ollivier and Zurek introduced the so-called quantum discord (QD), which is based on the fact that two equivalent ways to define the mutual information in classical world turn out to be inequivalent in the quantum ones, in order to quantify all nonclassical correlations among quantum systems[23]. And QD has been attracted much attention in many branches of physics. One important aspect is the relationship of QD with QPT[30–38]. Moreover, Werlang *et al.* found that QD can characterize exactly the critical points of the XXZ Heisenberg chain even at finite temperatures, while entanglement seems not[39]. Unfortunately, an analytical solution to QD is known only for typical two-qubit states. Subsequently, many distance-based quantum correlation measures have been proposed, such as geometric quantum discord defined via the Hilbert-Schmidt distance[24] (which may be changed by trivial local actions on the unmeasured party[25]) and its modified version via the Hellinger distance[26,27]. Another important version is the trace distance discord[28], which is defined through the Schatten one-norm. This quantum correlation exhibits some attractive features, and

[1]Institute of Signal Processing & Transmission, Nanjing University of Posts and Telecommunication, Nanjing, 210003, China. [2]National Laboratory of Solid State Microstructures & Innovation Center of Advanced Microstructures, Nanjing University, Nanjing, 210093, China. Correspondence and requests for materials should be addressed to W.W.C. (email: wwcheng@njupt.edu.cn) or J.-M.L. (email: liujm@nju.edu.cn)
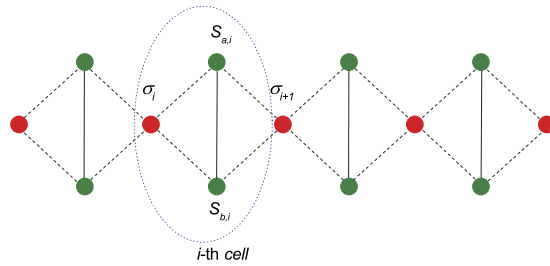
Figure 1. The schematic picture of Ising-XXZ diamond chain. The solid (dash) lines denote the Heienberg XXZ (Ising) interactions between two spins. The red (oliver) circles denote the Ising (Heisenberg) spins.

thus can be a physically meaningful measure. For instance, the trace distance obeys a contractive property, owing to the definition in terms of the Schatten one-norm, and this property is invariant under the unitary transformation. Recently, Ciccarello *et al.* showed that the trace distance discord can be analytically obtained for an arbitrary X state[29]. Taking account of the great success and flaw of previous quantum correlations in detecting QPT, it is meaningful to investigate the behavior of the trance distance discord for a typical quantum critical system, so that the capability and advantages of this measure to detect the QPT can be tested.

Regrading the QPT itself, the low-dimensional frustrated quantum spin models with competing interactions have attracted considerable attention due to their attractive quantum critical behaviours. For instance, the spin-1/2 quantum Heisenberg model with diamond chain structure is actively engaged in the investigations of geometric frustration[40–45]. Interestingly, this quantum spin model can be employed to explain the properties of some real materials such as azurite which has the 1/3 magnetization plateau and exhibits the double peaks in both magnetic susceptibility and specific heat[45]. On the other hand, the Ising-XXZ diamond model can also provide an excellent ground for rigorous study of pairwise quantum correlations at finite temperature in an infinite chain structure. The goal of this work is to check whether the trance distance discord as a measure can be used to describe the quantum critical behaviors in the spin diamond structure at finite temperature. The main properties of the quantum criticality(e.g., the finite-temperature scaling behavior, universality and critical exponents) will be visited both numerically and analytically.

Results

Ising-XXZ model and ground state phase diagram. The Ising-XXZ model with interstitial anisotropic Heisenberg spins and mixed nodal Ising spins on a diamond-structure chain in the presence of an external magnetic field is illustrated in Fig. 1. The Hamiltonian operator can be expressed as follows[40–44]:

$$H = \sum_{i=1}^{L} J(S_{a,i}, S_{b,i})_{\Delta} + J_1(S_{a,i}^z + S_{b,i}^z)(\sigma_i + \sigma_{i+1}) - h_0(S_{a,i}^z + S_{b,i}^z) - \frac{h}{2}(\sigma_i + \sigma_{i+1}) \tag{1}$$
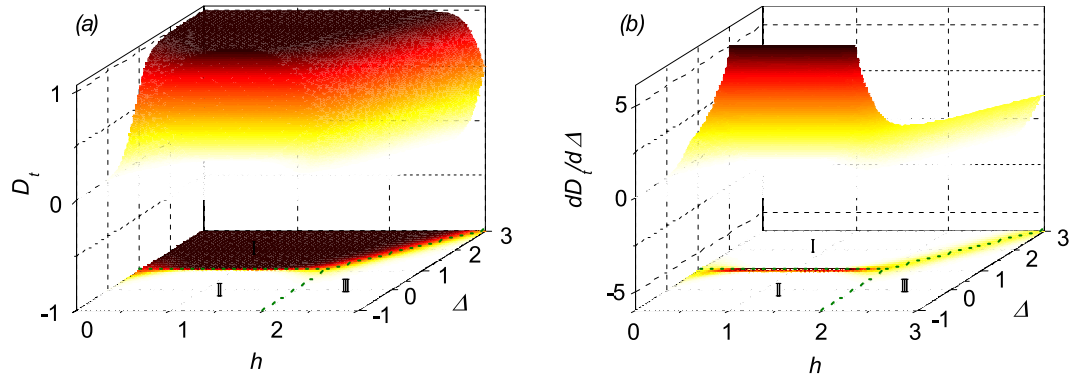
here, $(S_{a,i}, S_{b,i})_{\Delta} = S_{a,i}^x S_{b,i}^x + S_{a,i}^y S_{b,i}^y + \Delta S_{a,i}^z S_{b,i}^z$ denotes the Heisenberg dimer interaction, Δ is the anisotropy parameter, $S_{\alpha,i}$ stands for the quantum Heisenberg spin operators of the i-th cell along the chain, $\alpha = a,b$ numbers the two sites of the Heisenberg dimer, $S_{\alpha,i}^x, S_{\alpha,i}^y$ and $S_{\alpha,i}^z$ are three components of the Pauli operator, respectively. $\sigma_i = \pm 1$ denotes the classical Ising spin, while h and h_0 are the external magnetic fields acting on Ising spins and Heisenberg spins, respectively. The parameters J_1 and J correspond to the coupling constants of Ising interaction and XXZ interaction, respectively. For convenience, we set $J_1 = 1$, $J = 1$ and $h_0 = h$ throughout this work. L is the number of cells in the chain and will be treated as infinite. The Heisenberg spin coupling can be expressed using matrix notation as following,

$$(S_{a,i}, S_{b,i})_{\Delta} = \begin{pmatrix} \frac{\Delta}{4} & 0 & 0 & 0 \\ 0 & -\frac{\Delta}{4} & \frac{1}{2} & 0 \\ 0 & \frac{1}{2} & -\frac{\Delta}{4} & 0 \\ 0 & 0 & 0 & \frac{\Delta}{4} \end{pmatrix}. \tag{2}$$

By fixing the values for σ_i and σ_{i+1}, we can obtain the eigenstates in terms of basis $\{|\uparrow\uparrow\rangle, |\uparrow\downarrow\rangle, |\downarrow\uparrow\rangle, |\downarrow\downarrow\rangle\}$ given by,

$$|\psi_1\rangle = |\uparrow\uparrow\rangle, \tag{3a}$$

$$|\psi_2\rangle = \frac{1}{\sqrt{2}}(|\uparrow\downarrow\rangle + |\downarrow\uparrow\rangle), \tag{3b}$$

Figure 2. (**a**) The trance distance discord $\mathcal{D}_t$ and (**b**) its first-derivative $d\mathcal{D}_t/d\Delta$ with respect to Δ and h under temperature $T=0.1$. In the ENQ phase, the value of $\mathcal{D}_t$ almost equals to one and it approaches asymptotically to zero in the UFI and UFM phases at low temperature. Around the critical lines, $\Delta=1(h<2.0)$ and $\Delta-2h+3=0(h>2)$, and then the first-derivative $d\mathcal{D}_t/d\Delta$ exhibit a maximal, marking a QPT at finite temperature.

$$|\psi_3\rangle = \frac{1}{\sqrt{2}}(|\uparrow\downarrow\rangle - |\downarrow\uparrow\rangle), \tag{3c}$$

$$|\psi_4\rangle = |\downarrow\downarrow\rangle \tag{3d}$$

And the corresponding eigenvalues are $\lambda_1(\sigma_i,\sigma_{i+1})=\frac{\Delta}{4}+\left(1-\frac{h}{2}\right)(\sigma_i+\sigma_{i+1})-h$, $\lambda_2(\sigma_i,\sigma_{i+1})=\frac{1}{2}-\frac{\Delta}{4}-\frac{h}{2}(\sigma_i+\sigma_{i+1})$, $\lambda_3(\sigma_i,\sigma_{i+1})=-\frac{1}{2}-\frac{\Delta}{4}-\frac{h}{2}(\sigma_i+\sigma_{i+1})$, and $\lambda_4(\sigma_i,\sigma_{i+1})=\frac{\Delta}{4}-\left(1+\frac{h}{2}\right)(\sigma_i+\sigma_{i+1})+h$, respectively. In earlier work, three magnetic phases were observed (frustrated phase, ferrimagnetic phase and ferromagnetic phase) for the system[40]. In the present study, we take the tactic proposed by Rojas *et al.*, to re-arrange these phases into two main regions (entangled and unentangled)[41], which are closely related to the above three different magnetic phase, i.e., entangled state in the frustrated phase, $|ENT\rangle=\prod_{i=1}^{N}|\psi_3\rangle_i\otimes|\mu\rangle_i$, unentangled state in the ferrimagnetic phase $|UFI\rangle=\prod_{i=1}^{N}|\psi_1\rangle_i\otimes|-\rangle_i$, and unentangled state in the ferromagnetic phase $|UFM\rangle=\prod_{i=1}^{N}|\psi_1\rangle_i\otimes|+\rangle_i$. Here, $|\mu\rangle_i$ stands for an arbitrary value ($\mu=\pm1/2$) of the nodal spin in the ith block. According to the Bell states given in Eqs (3b) and (3c), at zero temperature the entangled state in the frustrated state is fully spanned at zero magnetic field, while the ferrimagnetic and ferromagnetic state are spanned by the unentangled states, respectively. The eigenvalues for the UFM is given by $E_{UFM}=1+\Delta/4-3h/2$ and the eigenvalue for UFI state is $E_{UFI}=-1+\Delta/4-h/2$. The entangled state (quantum ferrimagnetic state), denoted by $|ENQ\rangle=\prod_{i=1}^{N}|\psi_3\rangle_i\otimes|+\rangle_i$, has its eigenvalue $E_{ENQ}=-1/2-\Delta/4-h/2$. Thus, the boundary between these critical phases at zero temperature can be exactly figured out according to these eigenvalues.

Trace distance and QPT at finite temperature. It is noted that the thermal entanglement for such a model on different critical phases was once discussed in the previous works[41–44]. The results showed that the entanglement may disappear as temperature exceeds a threshold T_c, making the entanglement fail to characterize the critical points above the critical temperature. Here we focus on the relationship between the trace distance discord and the quantum critical phenomenon at finite temperature. Without loss of generality, we plot the $\mathcal{D}_t$ as a function of Δ and h for a fixed finite temperature $T=0.1$ as an example in Fig. 2(a). Obviously, one can see that the UFI and ENQ regions (or phases) are separated by line $\Delta=1$ with $h<2$, and the UFM and ENQ regions (or phases) are separated by line $\Delta-2h+3=0$ with $h>2$. The trance distance discord almost equals to one in the ENQ region and approaches to zero in the other two regions. Around the boundary between the unentangled state and entangled one, the trace distance discord falls quickly and approaches to zero asymptotically. Here it should be mentioned that the quantum state for Heisenberg dime is the unentangled state $|\psi_1\rangle$ and thus all quantum correlations(concurrence, quantum discord, trace distance discord, etc.) equal to zero when the system is in the UFI or UFM phase. In the other words, these is no change for these correlations when the system goes across the critical line between the two phases. In Fig. 2(b), we plot the first-derivative of $\mathcal{D}_t$ with respect to Δ for the fixed finite temperature $T=0.1$. Again and obviously, the maximal appears around the critical lines. It is known that the first-derivative with respect to the driving parameter shows an extremal behavior near these critical lines and will be divergent in the thermodynamic limit $T\to0$.

To this stage, one is convinced that these properties of the trance distance discord indeed can reveal the critical regions at finite temperature for this model. In the following, we shall proceed to perform quantitative analysis on the $\mathcal{D}_t$ around the critical lines at finite temperature.

Quantum criticality from ENQ to UFI. Given the discussion above, it is clear that there exists a transition from ENQ phase to UFI phase around line $\Delta=1$ with $h\leq2$. In Fig. 3(a) is plotted the the density of $\mathcal{D}_t$ as a func-
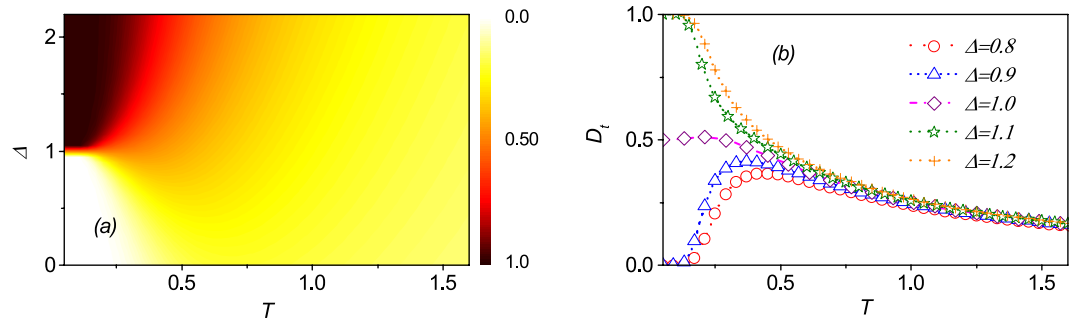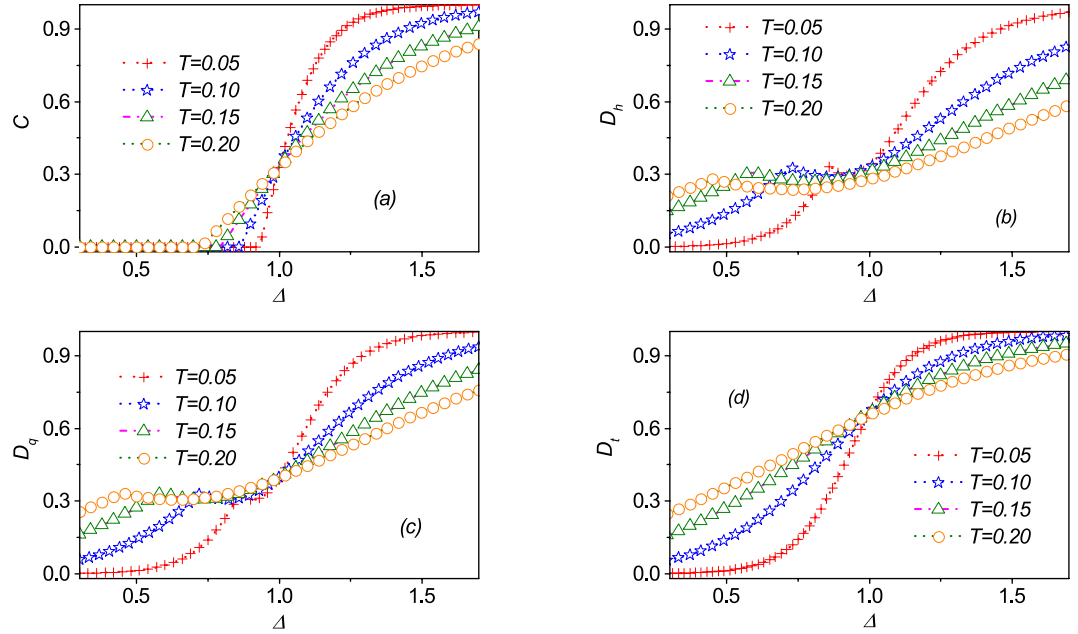
Figure 3. (**a**) The trance distance discord $\mathcal{D}_t$ as a function of T and Δ. (**b**) The trance distance discord $\mathcal{D}_t$ as a function of T at different values of parameter Δ.
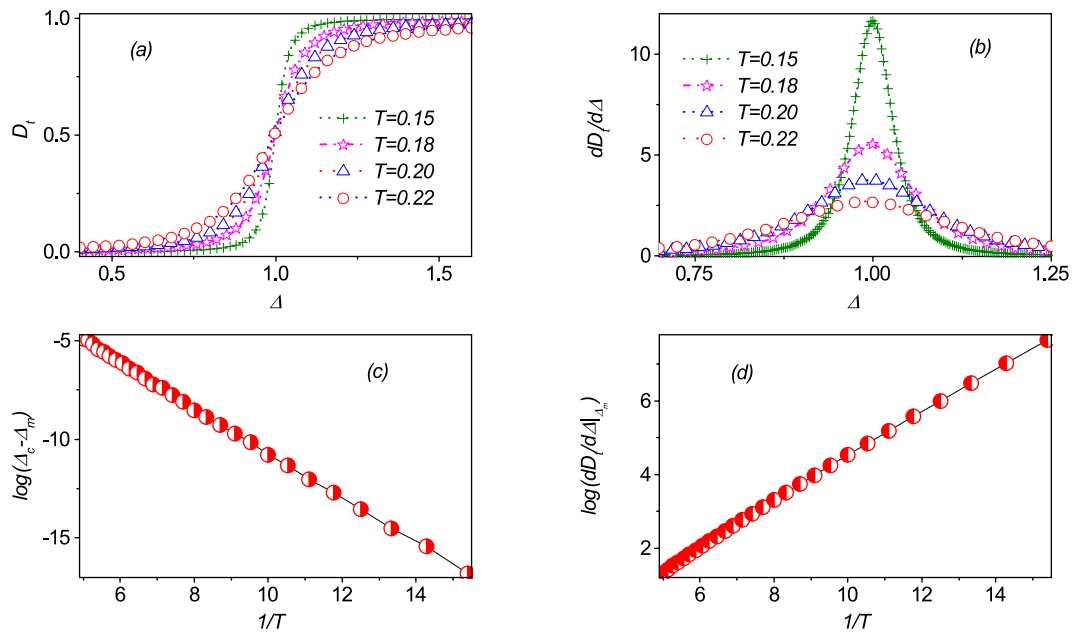
Figure 4. The calculated $\mathcal{D}_t$ (**a**) and its first-derivative $d\mathcal{D}_t/d\Delta$ (**b**) as a function of parameter Δ around the critical point $\Delta = 1.0$. (**c**) The peak position Δ_m can be regarded as a pseudo-critical point which shifts with increasing temperature T following relationship $\log(\Delta_c - \Delta_m) = k_1 \frac{1}{T} + const$ in approaching to the critical point Δ_c. This behavior implies that $\Delta_m \to \Delta_c$ as $T \to 0$. (**d**) The maximum value of $d\mathcal{D}_t/d\Delta$ at the pseudocritical point Δ_m as a function of T.

tion of T and Δ for a fixed $h = 1$. Clearly $\mathcal{D}_t$ does not equal to zero over the whole parameter region and it is finite even at high temperature where the entanglement may disappear[41,44]. As addressed above, the reason is that $\mathcal{D}_t$ can measure the total quantum correlations of a state ρ while the entanglement can only reflect part of them. This property of $\mathcal{D}_t$ makes it possible to detect the quantum critical point at finite temperature. We also note that $\mathcal{D}_t$ may increase with temperature in a given region, which is very similar to QD in the Heisenberg XYZ model[46]. Naturally, this character tends to disappear as temperature goes too high. In Fig. 3(b), $\mathcal{D}_t$ as a function of temperature T for several different values of Δ are plotted. Obviously, for $\Delta > 1$, D_t decreases monotonically with increasing T and approaches to zero asymptotically in the high temperature region. However, for $\Delta < 1$, $\mathcal{D}_t$ almost equals to zero in the low temperature region, and then increases up to a maximal before going down to zero asymptotically as T increases further. These results also indicate that there indeed exists a transition when the system goes across $\Delta = 1$.

To explore the effect of finite-temperature on $\mathcal{D}_t$, we present the calculated $\mathcal{D}_t$ as a function of Δ at several temperatures T around the point $\Delta = 1.0$ in Fig. 4(a). $\mathcal{D}_t$ increases monotonically with increasing Δ and this trend becomes more significant as temperature T is lower. We plot the first-derivative of $\mathcal{D}_t$ with respect to Δ in Fig. 4(b) to reflect such trend. The $d\mathcal{D}_t/d\Delta$ exhibits a clear singularity around the critical point $\Delta = 1.0$ in the limit $T \to 0$. Generally speaking, the appearance of nonanalytic behavior of a physical quantity is fundamentally a feature of QPT. It is accompanied with a scaling behavior due to the divergency of the correlation length. Fig. 4(b) shows the shift of the anomaly position, marked by the sharp peak, and the peak height with increasing

Figure 5. Several typical quantum correlations, (**a**) concurrence $\mathcal{C}$, (**b**) Hellinger distance $\mathcal{D}_h$, (**c**) quantum discord $\mathcal{D}_q$, and (**d**) trance distance discord $\mathcal{D}_t$ as a function of parameter Δ around the points$(\Delta,h) = (1,0)$ at various temperatures T, respectively. Obviously, they are all smooth functions of Δ. However, the first-derivatives for $\mathcal{C}$, $\mathcal{D}_q$ and $\mathcal{D}_h$ would exhibit an unexpected discontinuity point Δ_f, which is unfortunately not a real critical point except normal discontinuity point Δ_c for the QPT.

temperature. In details, the peak position Δ_m can be regarded as a pseudo-critical point which shifts with temperature T following the scaling law:

$$\log(\Delta_c - \Delta_m) = k_1 \frac{1}{T} + const. \tag{4}$$

The numerical results are plotted in Fig. 4(c), implying $\Delta_m \to \Delta_c$ as $T \to 0$. On the other aspect, the value of the derivative of $\mathcal{D}_t$ is logarithmically divergent at the pseudo-critical point Δ_m in the thermodynamic limit,

$$\log(d\mathcal{D}_t/d\Delta|_{\Delta_m}) = k_2 \frac{1}{T} + const. \tag{5}$$

The numerical results are plotted in Fig. 4(d), suggesting that $d\mathcal{D}_t/d\Delta$ shows a singularity at the critical point as temperature approaches to zero.

As a comparison, it is rather interesting to check the behaviors of some other typical quantum correlations around the critical point. In Fig. 5(a), we plot concurrence $\mathcal{C}$ as a function of Δ at several different temperatures T with $h = 0$. Although the $\mathcal{C} \sim \Delta$ curves are continuous, there would exist two points where the corresponding first-derivative ($d\mathcal{C}/d\Delta$) is continuous instead of divergent. The discontinuity at $\Delta_c = 1$ does indicate the QPT of the present model. However, the unexpected discontinuity occurs at Δ_f where entanglement $\mathcal{C}$ disappears, suggesting that this is a false critical point. This behavior for entanglement $\mathcal{C}$ is very similar to the counterpart in the XX spin model with multi-site interaction[18]. It is known that the origin of nonanalyticity in the concurrence at Δ_f comes from the requirement that the concurrence should be non-negative instead from the nonanalyticity of ρ. Therefore, the discontinuity in $d\mathcal{C}/d\Delta$ does not necessarily indicate the existence of QPT. In Fig. 5(b) and (c), dependences of Hellinger distance $\mathcal{D}_h$ and quantum discord $\mathcal{D}_q$ on Δ at several temperatures with $h = 0$ are plotted. Obviously, both of them exhibit a cuspate behavior when the anisotropy parameter Δ increases. These phenomena cannot appear under the influence of magnetic field. For the QD, such phenomena can be also observed in other models[46]. Thus we see that the first derivative of these quantum correlations would show discontinuities at both points $\Delta_c = 1$ and Δ_p. The discontinuity at $\Delta_c = 1$ does indicate the QPT of the present model. However, the unexpected discontinuity point occurring at Δ_p is not a real critical one. In comparison with the behaviors of above typical quantum correlations, we also plot the trance distance discord in Fig. 5(d). Obviously, the $\mathcal{D}_t \sim \Delta$ curve is continuous and smooth, and we can anticipate that there would be one point where the first derivative of $\mathcal{D}_t$ is discontinuous as temperature approaches to zero, marking the critical point exactly. Therefore, we can reasonably state that the trace distance, in contrast to other quantum correlations (e.g., concurrence, quantum discord and Hellinger distance), may be more reliable to spotlight the critical points for this model under certain situations at finite temperature.
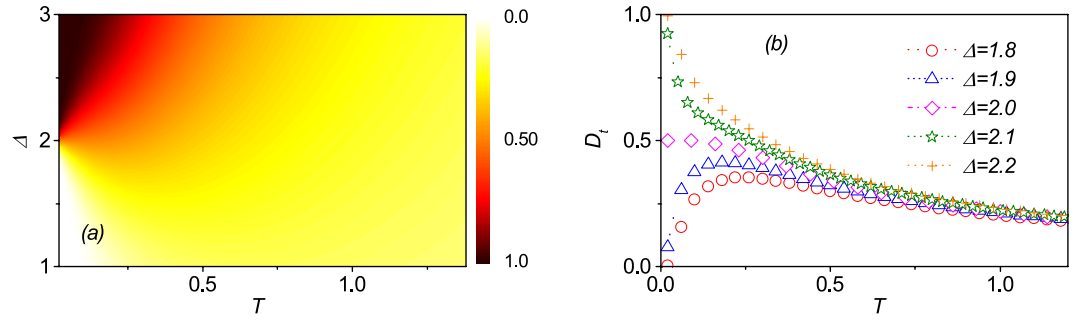
Figure 6. (**a**) The trance distance discord $\mathcal{D}_t$ as a function of T and Δ. (**b**) The trance distance discord $\mathcal{D}_t$ as a function of T at several different values of parameter Δ.
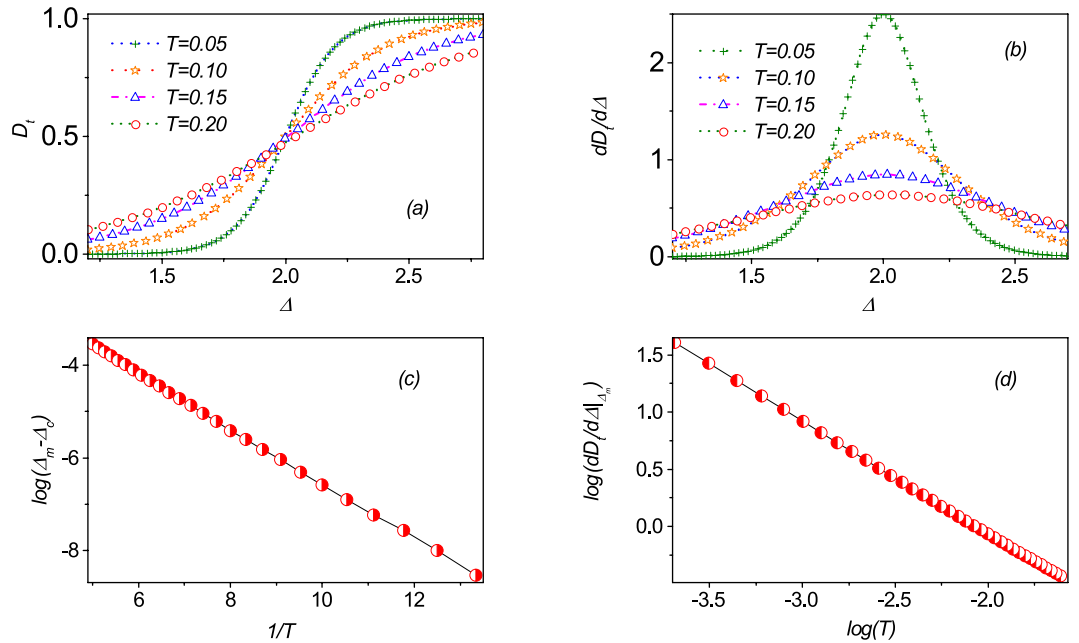
Figure 7. (**a**) $\mathcal{D}_t$ and (**b**) its first-derivative $d\mathcal{D}_t/d\Delta$ as a function of parameters Δ, respectively, around the critical line $\Delta - 2h + 3 = 0$. (**c**) The peak position Δ_m can be regarded as a pseudo-critical point which shifts with temperature T following relation $\log(\Delta_c - \Delta_m) = k_2 \frac{1}{T} + const$ in approaching to the critical point Δ_c. This character implies $\Delta_m \to \Delta_c$ as $T \to 0$. (**d**) The maximal value of $d\mathcal{D}_t/d\Delta$ at the pseudocritical point Δ_m as a function of T. The scaling behavior is very different from the counterpart in the quantum criticality from ENQ to UFI.

Quantum criticality from ENQ to UFM. Based on the above discussion, one understands that there exists another transition from ENQ phase to UFM phase around critical line $\Delta - 2h + 3 = 0$ with $h > 2$. Figure 6(a) and (b) present the $\mathcal{D}_t$ as a function of parameters Δ and T for a fixed external field $h = 2.5$. The $\mathcal{D}_t$ pattern is very similar to the counterpart around critical line $\Delta = 1$ with $h < 2$. For instance, $\mathcal{D}_t$ decreases monotonically with increasing T and approaches to zero at high temperature when $\Delta > 2.0$. For $\Delta < 2.0$, $\mathcal{D}_t$ is nearly zero in the low temperature limit, but increases rapidly to a maximal and then falls gradually down to zero again with increasing T. These results also suggest that the system undergoes a QPT as parameters Δ or h pass across the critical line $\Delta - 2h + 3 = 0$ with $h > 2$ at finite temperature.

To further understand the properties of $\mathcal{D}_t$ around the critical line $\Delta - 2h + 3 = 0$, we investigate the finite-temperature scaling behavior quantitatively. In Fig. 7(a), we present $\mathcal{D}_t$ with respect to Δ around the point $(\Delta, h) = (2.0, 2.5)$ at different temperatures T. $\mathcal{D}_t$ increases monotonically with increasing Δ and this dependence becomes more significant at lower temperature T. To characterize this dependence, we also plot the first-derivative of $\mathcal{D}_t$ with respect to Δ in Fig. 7(b), and a singularity around the critical point $(\Delta, h) = (2.0, 2.5)$ in the limit $T \to 0$ is displayed. One also observes that the peak position marking the anomaly shifts and the peak height decreases with increasing temperature, and the peak position Δ_m as a pseudo-critical point can be described by the following scaling law:
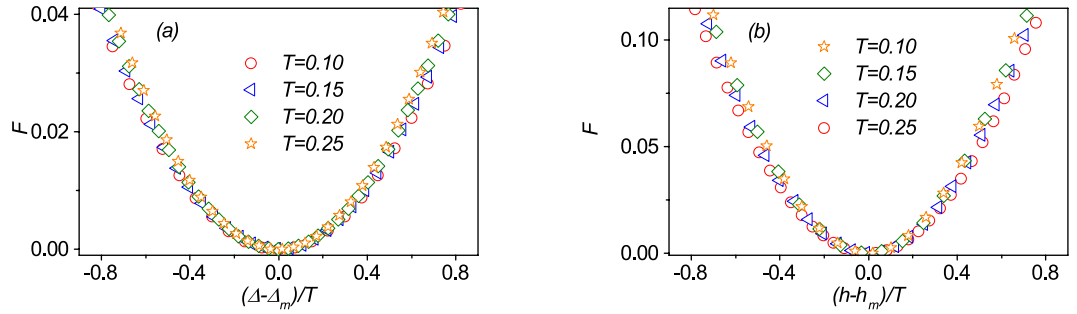
Figure 8. (**a**) The evaluated $F = [1 - \exp(d\mathcal{D}_t/d\Delta - d\mathcal{D}_t/d\Delta|_{\Delta_m})]$ as a function of $(\Delta - \Delta_m)/T$ at different temperatures. (**b**) The evaluated $F = [1 - \exp(d\mathcal{D}_t/dh - d\mathcal{D}_t/dh|_{h_m})]$ as a function of $(h - h_m)/T$ at different temperatures. Given the fixed parameter $h = 2.5$ (**a**) or $\Delta = 2$ (**b**), all the data collapse on a single curve, respectively, as expected from the finite temperature scaling ansatz.

$$\log(\Delta_c - \Delta_m) = k_3\frac{1}{T} + const \qquad (6)$$

in approaching to the critical point Δ_c. The numerical results are plotted in Fig. 7(c), implying $\Delta_m \to \Delta_c$ as $T \to 0$. On the other hand, at the pseudo-critical point Δ_m, the value $d\mathcal{D}_t/d\Delta$ diverges logarithmically with decreasing temperature T, according to

$$\log(d\mathcal{D}_t/d\Delta|_{\Delta_m}) = k_4 \log(T) + const. \qquad (7)$$

The numerical results are plotted in Fig. 7(d). Here, it should be mentioned that the scaling behaviors are very different from the counterpart in the quantum criticality from ENQ phase to UFI phase. The two kinds of transitions can be distinguished by the different finite-temperature scaling behaviors.

Furthermore, by proper scaling and taking into account the distance of the maximum of $d\mathcal{D}_t/d\Delta$ from the critical point, all the data at different temperatures can be properly re-scaled onto the single curve using the scaling transform relation: $F = [1 - \exp(d\mathcal{D}_t/d\Delta - d\mathcal{D}_t/d\Delta|_{\Delta_m})]$ against $(\Delta - \Delta_m)/T^{\frac{1}{\nu}7}$. The results around the point $(\Delta, h) = (2, 2.5)$ are plotted in Fig. 8(a), demonstrating the scaling of the critical behaviors. The critical exponent $\nu = 1$ is obtained.

We understand that the transitions across the critical line $\Delta - 2h + 3 = 0$ can be driven by Δ or h. It is also well known that the most important ingredient of physics with quantum phase transitions is the universality class, which means that different driving parameters may exhibit the same behavior around the critical point and thus have the same critical exponent[1]. To check this universality behavior, we investigate the scaling behaviors given different values of driving parameter, i.e., external field h. In our calculations, we find that they do exhibit similar behaviors. We ignore the details and only focus on the results from which the critical exponent can be extracted. By proper scaling treatment and taking into account the distance of the maximal point of $d\mathcal{D}_t/dh$ from the critical point, we plot the scaling function $F = [1 - \exp(d\mathcal{D}_t/dh - d\mathcal{D}_t/dh|_{h_m})]$ against $(h - h_m)/T^{\frac{1}{\nu}}$ for different temperatures T around the point $(\Delta, h) = (2, 2.5)$ in Fig. 8(b). Obviously, all the data collapse onto a single curve, confirming the scaling behavior. The extracted critical exponent is $\nu = 1$. These results also demonstrate convincingly that the quantum critical behaviors can be characterized by the trace distance even at nonzero (finite) temperature.

Discussion

Here the quantum criticality in the Ising-XXZ diamond structure at finite temperature have been studied by the trance distance discord calculations. Around the critical lines, the first-order derivative of the trace distance discord exhibits a maximal at a finite temperature and diverges under the thermodynamic limits $T \to 0$. By analyzing the finite-temperature scaling behaviors, we show that the trace distance discord can detect exactly the quantum phase transition from the entangled state in ferrimagnetic phase to an unentangled state in ferrimagnetic phase or to an unentangled state in ferromagnetic phase. The results also show that the trace distance can distinguish the two kinds of transitions by consulting to the different finite-temperature scaling behaviors. As a comparison, we also study the behaviors of some other typical quantum correlations (e.g., concurrence, quantum discord and Hellinger distance) around the critical points, and the results state that the trace distance discord is more reliable than the others to spotlight the critical points for this Ising-XXZ diamond structure at finite temperatures.

Surely, this model system has three different critical phases, and it would be significant and challenging in the future to consider the multipartite quantum correlations which may grasp all these transitions. The bipartite quantum correlations imposed on this Ising-XXZ diamond structure, as studied in this work, can not detect the transition from UFI phase to UFM phase at finite temperature, an issue for future investigations.

Methods

By employing the transfer-matrix method, the reduced density operator for the Heisenberg spin pairs can be obtained exactly[41],

$$\rho = \begin{pmatrix} \rho_{11} & 0 & 0 & 0 \\ 0 & \rho_{22} & \rho_{23} & 0 \\ 0 & \rho_{32} & \rho_{33} & 0 \\ 0 & 0 & 0 & \rho_{44} \end{pmatrix} \tag{8}$$

with

$$\rho_{i,j} = \frac{\rho_{ij}\left(\frac{1}{2}, \frac{1}{2}\right) + \rho_{ij}\left(-\frac{1}{2}, -\frac{1}{2}\right)}{2\Lambda} + \frac{2\rho_{ij}\left(\frac{1}{2}, -\frac{1}{2}\right)\tau_{+-}}{Q\Lambda} + \frac{\left[\rho_{ij}\left(\frac{1}{2}, \frac{1}{2}\right) - \rho_{ij}\left(-\frac{1}{2}, -\frac{1}{2}\right)\right](\tau_{++} - \tau_{--})}{2Q\Lambda}. \tag{9}$$

Here, $\Lambda = (\tau_{++} + \tau_{--} + Q)/2$, $Q = [(\tau_{++} - \tau_{--})^2 + 4\tau_{+-}^2]^{\frac{1}{2}}$, $\tau(\sigma_i, \sigma_{i+1}) = \sum_{n=1}^{4} \exp[-\beta\lambda_n(\sigma_i, \sigma_{i+1})]$ with $\tau_{++} = \tau\left(\frac{1}{2}, \frac{1}{2}\right), \tau_{+-} = \tau\left(\frac{1}{2}, -\frac{1}{2}\right), \tau_{-+} = \tau\left(-\frac{1}{2}, \frac{1}{2}\right), \tau_{--} = \tau\left(-\frac{1}{2}, -\frac{1}{2}\right)$ and $\beta = 1/k_B T$. T is the absolute temperature and k_B can be taken as a unit. $\rho_{ij}(\sigma_r, \sigma_{r+1})$ are given by,

$$\rho_{11}(\sigma_r, \sigma_{r+1}) = e^{-\beta\lambda_1(\sigma_r\sigma_{r+1})},$$
$$\rho_{22}(\sigma_r, \sigma_{r+1}) = \frac{1}{2}(e^{-\beta\lambda_2(\sigma_r\sigma_{r+1})} + e^{-\beta\lambda_3(\sigma_r\sigma_{r+1})}),$$
$$\rho_{23}(\sigma_r, \sigma_{r+1}) = \frac{1}{2}(e^{-\beta\lambda_2(\sigma_r\sigma_{r+1})} - e^{-\beta\lambda_3(\sigma_r\sigma_{r+1})}),$$
$$\rho_{44}(\sigma_r, \sigma_{r+1}) = e^{-\beta\lambda_4(\sigma_r\sigma_{r+1})} \tag{10}$$

For a bipartite system described by the density operator ρ_{AB}, the trance distance discord is defined as[28,29]

$$\mathcal{D}_t = \min_{\chi \in \rho_{CQ}} \|\rho_{AB} - \chi\|_1, \tag{11}$$

where $\|\rho_{AB} - \chi\|_1 = Tr\sqrt{(\rho_{AB} - \chi)^\dagger(\rho_{AB} - \chi)}$ denotes the trace distance between ρ_{AB} and $\chi \in \rho_{CQ}$, and

$$\rho_{CQ} = \sum_k p_k \Pi_k^A \otimes \rho_k^B, \tag{12}$$

$\{p_k\}$ is the probability distribution, and Π_k^A and ρ_k^B are the orthogonal projector for A and the density operator for B, respectively. For a two-qubit X state ρ, which only contains nonzero elements along the main diagonal and anti-diagonal, the calculation of the trace distance discord can be simplified by[29]

$$\mathcal{D}_t = \left[\frac{\gamma_1^2 \max\{\gamma_3^2, \gamma_2^2 + \chi_3^2\} - \gamma_2^2 \min\{\gamma_1^2, \gamma_3^2\}}{\max\{\gamma_3^2, \gamma_2^2 + \chi_3^2\} - \min\{\gamma_1^2, \gamma_3^2\} + \gamma_1^2 - \gamma_2^2}\right]^{\frac{1}{2}}, \tag{13}$$

here, $\gamma_{1,2} = 2(|\rho_{23}| \pm |\rho_{14}|), \gamma_3 = 1 - 2(\rho_{22} + \rho_{33})$, and $\chi_3 = 2(\rho_{11} + \rho_{22}) - 1$.

References

1. Sachdev, S. *Quantum Phase Transition* (Cambridge University Press, Cambridge, UK, 1999).
2. Kopp, A. & Chakravarty, S. Criticality in correlated quantum matter. *Nature Physics* **1,** 53 (2005).
3. Yang, Z. H., Yang, L. P., Dai, J. H. & Xiang, T. Rigorous solution of the spin-1 quantum Ising model with single-ion anisotropy. *Phys. Rev. Lett.* **100,** 067203 (2008).
4. Coleman, P. & Schofield, A. J. Quantum criticality. *Nature* **433,** 226 (2005).
5. Shan, C. J., Cheng, W. W., Liu, J. B., Cheng, Y. S. & Liu, T. K. Scaling of geometric quantum discord close to a topological phase transition. *Sci. Rep.* **4,** 4473 (2014).
6. Liu, X. M., Cheng, W. W. & Liu, J.-M. Renormalization-group approach to quantum fisher information in an XY model with staggered dzyaloshinskii-moriya interaction. *Sci. Rep.* **6,** 19359 (2016).
7. Osterloh, A., Amico, L., Falci, G. & Fazio, R. Scaling of entanglement close to a quantum phase transition. *Nature* **416,** 608 (2002).
8. Osborne, T. J. & Nielsen, M. A. Entanglement in a simple quantum phase transition. *Phys. Rev. A* **66,** 032110 (2002).
9. Vidal, G., Latorre, J. I., Rico, E. & Kitaev, A. Entanglement in quantum critical phenomena. *Phys. Rev. Lett.* **90,** 227902 (2003).
10. Syljuåsen, O. F. Entanglement and spontaneous symmetry breaking in quantum spin models. *Phys. Rev. A* **68,** 060301 (2003).
11. Gu, S.-J., Lin, H.-Q. & Li, Y.-Q. Entanglement, quantum phase transition, and scaling in the XXZ chain. *Phys. Rev. A* **68,** 042330 (2003).
12. Glaser, U., Büttner, H. & Fehske, H. Entanglement and correlation in anisotropic quantum spin systems. *Phys. Rev. A* **68,** 032318 (2003).
13. Wu, L.-A., Sarandy, M. S. & Lidar, D. A. Quantum phase transitions and bipartite entanglement. *Phys. Rev. Lett.* **93,** 250404 (2004).
14. Vidal, J., Palacios, G. & Mosseri, R. Entanglement in a second-order quantum phase transition. *Phys. Rev. A* **69,** 022107 (2004).
15. Somma, R., Ortiz, G., Barnum, H., Knill, E. & Viola, L. Nature and measure of entanglement in quantum phase transitions. *Phys. Rev. A* **70,** 042311 (2004).
16. Amico, L., Osterloh, A., Plastina, F., Fazio, R. & Massimo Palma, G. Dynamics of entanglement in one-dimensional spin systems. *Phys. Rev. A* **69,** 022304 (2004).
17. Verstraete, F., Popp, M. & Cirac, J. I. Entanglement versus correlations in spin systems. *Phys. Rev. Lett.* **92,** 027901 (2004).

18. Yang, M.-F. Reexamination of entanglement and the quantum phase transition. *Phys. Rev. A* **71**, 030302 (2005).
19. Amico, L. & Patanè, D. Entanglement crossover close to a quantum critical point. *EPL* **77**, 17001 (2007).
20. Justino, L. & de Oliveira, T. R. Bell inequalities and entanglement at quantum phase transitions in the *XXZ* model. *Phys. Rev. A* **85**, 052128 (2012).
21. Li, Y.-C. & Lin, H.-Q. Quantum coherence and quantum phase transitions. *Sci. Rep.* **6**, 26365 (2016).
22. Qin, M., Ren, Z.-Z. & Zhang, X. Universal quantum correlation close to quantum critical phenomena. *Sci. Rep.* **6**, 26042 (2016).
23. Ollivier, H. & Zurek, W. H. Quantum discord: A measure of the quantumness of correlations. *Phys. Rev. Lett.* **88**, 017901 (2001).
24. Dakić, B., Vedral, V. & Brukner, C. Necessary and sufficient condition for nonzero quantum discord. *Phys. Rev. Lett.* **105**, 190502 (2010).
25. Piani, M. Problem with geometric discord. *Phys. Rev. A* **86**, 034101 (2012).
26. Chang, L. & Luo, S. Remedying the local ancilla problem with geometric discord. *Phys. Rev. A* **87**, 062303 (2013).
27. Girolami, D., Tufarelli, T. & Adesso, G. Characterizing nonclassical correlations via local quantum uncertainty. *Phys. Rev. Lett.* **110**, 240402 (2013).
28. Paula, F. M., de Oliveira, T. R. & Sarandy, M. S. Geometric quantum discord through the schatten 1-norm. *Phys. Rev. A* **87**, 064101 (2013).
29. Ciccarello, F., Tufarelli, T. & Giovannetti, V. Toward computability of trace distance discord. *New Journal of Physics* **16**, 013038 (2014).
30. Dillenschneider, R. Quantum discord and quantum phase transition in spin chains. *Phys. Rev. B* **78**, 224413 (2008).
31. Sarandy, M. S. Classical correlation and quantum discord in critical systems. *Phys. Rev. A* **80**, 022108 (2009).
32. Maziero, J., Guzman, H. C., Céleri, L. C., Sarandy, M. S. & Serra, R. M. Quantum and classical thermal correlations in the *XY* spin-$\frac{1}{2}$ chain. *Phys. Rev. A* **82**, 012106 (2010).
33. Li, Y.-C. & Lin, H.-Q. Thermal quantum and classical correlations and entanglement in the *XY* spin model with three-spin interaction. *Phys. Rev. A* **83**, 052323 (2011).
34. Rulli, C. C. & Sarandy, M. S. Global quantum discord in multipartite systems. *Phys. Rev. A* **84**, 042109 (2011).
35. Tomasello, B., Rossini, D., Hamma, A. & Amico, L. Ground-state factorization and correlations with broken symmetry. *EPL* **96**, 27002 (2011).
36. Modi, K., Brodutch, A., Cable, H., Paterek, T. & Vedral, V. The classical-quantum boundary for correlations: Discord and related measures. *Rev. Mod. Phys.* **84**, 1655–1707 (2012).
37. Campbell, S., Richens, J., Gullo, N. L. & Busch, T. Criticality, factorization, and long-range correlations in the anisotropic XY model. *Phys. Rev. A* **88**, 062305 (2013).
38. Huang, Y. Scaling of quantum discord in spin models. *Phys. Rev. B* **89**, 054410 (2014).
39. Werlang, T., Trippe, C., Ribeiro, G. A. P. & Rigolin, G. Quantum correlations in spin chains at finite temperatures and quantum phase transitions. *Phys. Rev. Lett.* **105**, 095702 (2010).
40. Ananikian, N. S., Ananikyan, L. N., Chakhmakhchyan, L. A. & Rojas, O. Thermal entanglement of a spin-1/2 Ising-heisenberg model on a symmetrical diamond chain. *J. Phys.: Condens. Matter* **24**, 256001 (2012).
41. Rojas, O., Rojas, M., Ananikian, N. S. & de Souza, S. M. Thermal entanglement in an exactly solvable Ising-*XXZ* diamond chain structure. *Phys. Rev. A* **86**, 042330 (2012).
42. Rojas, M., de Souza, S. M. & Rojas, O. Rise of pairwise thermal entanglement for an alternating Ising and heisenberg spin chain in an arbitrarily oriented magnetic field. *Phys. Rev. A* **89**, 032336 (2014).
43. Sterćka, J., Rojas, O., Verkholyak, T. & Lyra, M. L. Magnetization process, bipartite entanglement, and enhanced magnetocaloric effect of the exactly solved spin-1/2 Ising-heisenberg tetrahedral chain. *Phys. Rev. E* **89**, 022143 (2014).
44. Gao, K., Xu, Y. L., Kong, X. M. & Liu, Z. Q. Thermal quantum correlations and quantum phase transitions in Ising-XXZ diamond chain. *Physica A* **429**, 10 (2015).
45. Rule, K. C. *et al.* Nature of the spin dynamics and 1/3 magnetization plateau in azurite. *Phys. Rev. Lett.* **100**, 117202 (2008).
46. Werlang, T. & Rigolin, G. Thermal and magnetic quantum discord in heisenberg models. *Phys. Rev. A* **81**, 044101 (2010).

Acknowledgements

Author Contributions

W.W.C. proposed the idea. W.W.C and X.Y.W carried out the calculations. Y.B.S., L.Y.G., S.M.Z. and J.M.L commented the model. W.W.C and J.M.L wrote the paper. All authors discussed the results and commented on the manuscript.

Additional Information

Competing financial interests: The authors declare no competing financial interests.

How to cite this article: Cheng, W. W. *et al.* Finite-temperature scaling of trace distance discord near criticality in spin diamond structure. *Sci. Rep.* **7**, 42360; doi: 10.1038/srep42360 (2017).

Publisher's note: Springer Nature remains neutral with regard to jurisdictional claims in published maps and institutional affiliations.